Irma Slowik, Axel Fischer, Stefan Gutsche, Robert Brückner, Hartmut Fröb, Simone Lenk, Sebastian Reineke, Karl Leo

New concept for organic lightemitting devices under high excitations using emission from a metal-free area

Erstveröffentlichung in / First published in:

SPIE Photonics Europe. Brussels, 2016. Bellingham: SPIE, Vol. 9895 *[Zugriff am: 23.05.2019].*

DOI: https://doi.org/10.1117/12.2228233

New concept for organic light-emitting devices under high excitations using emission from a metal-free area

Irma Slowik, Axel Fischer, Stefan Gutsche, Robert Brückner, Hartmut Fröb, et al.

Irma Slowik, Axel Fischer, Stefan Gutsche, Robert Brückner, Hartmut Fröb, Simone Lenk, Sebastian Reineke, Karl Leo, "New concept for organic light-emitting devices under high excitations using emission from a metal-free area," Proc. SPIE 9895, Organic Photonics VII, 989507 (27 April 2016); doi: 10.1117/12.2228233

SPIE.

Event: SPIE Photonics Europe, 2016, Brussels, Belgium

Invited Paper

New concept for organic light-emitting devices under high excitations using emission from a metal-free area

Irma Slowik, Axel Fischer, Stefan Gutsche, Robert Brückner, Hartmut Fröb, Simone Lenk, Sebastian Reineke, and Karl Leo

Technische Universtität Dresden, Institut für Angewandte Photophysik, Georg-Bähr-Strasse-1, Dresden, Germany

ABSTRACT

In this work, a new organic light-emitting device (OLED) structure is proposed that allows light-emission from a metal-free device region, thus reducing the hurdles towards an electrically pumped organic solid state laser (OSL). Our design concept employs a stepwise change from a highly conductive but opaque metal part to a highly transparent but less conductive intrinsic emission layer. Here, the high current densities are localized to an area of a few micrometer in square, which is in the range of the mode volume of the transverse mode of an organic vertical-cavity surface-emitting laser (VCSEL). Besides these experimental results, we present findings from simulations which further support the feasibility of our design concept. Using an equivalent circuit approach, representing the current flow in the device, we calculate the time-dependent length of the emission zone and give estimations for appropriate material parameters.

Keywords: Organic semiconductor, Organic light emitting device, organic solid state laser, equivalent circuit model, lateral emission, current density distribution, high excitation

1. INTRODUCTION

In the last decades, organic light-emitting devices (OLEDs) have been studied extensively. Because of their promising properties such as high electroluminescence efficiency, flexibility, light weight and low manufacturing cost, they found various applications such as flat-panel displays and solid-state lighting.[1,2] Nowadays, highly conductive transport layers are used reducing injection barriers allowing low operation voltages.[3–5] In this so called pin-OLEDs, vertical current transport works efficiently within the stack of about 100 nm.
Nevertheless, operating OLEDs at high excitation stays a major challenge due to the influence of various exciton quenching mechanism,[6,7] resulting in a reduction of the external quantum-efficiency known as efficiency roll-off.[8] Furthermore, Joule heating caused by high current results in the thermal breakdown of the device.[9–11] However, reaching high current densities is a key prerequisite towards electrically pumped organic semiconductor lasers (OSL), since high exciton densities have to be realized within the lifetime of the light-emitting states. Hence, OLEDs, which can sustain high current densities in the range of 1 kA/cm^2 are an important step for the development of an electrically driven OSL.[12–14] To reduce the external quantum-efficiency roll-off at high current densities nanopatterning, of the OLED active area had been used recently.[15–18] Joule heating of the devices can be decreased by short pulse excitation[7,19,20] as well as the usage of high thermally conducting substrates.[10] Even so, driving OLEDs at high excitation above the lasing threshold[15] have never been reached.
Furthermore, for the realization of an electrically pumped OSL, the OLED structure get optical feedback by e.g.an optical microcavity. Because of the low electrical conductivity of organic semiconductors, metal contacts are required for the injection of high current densities. Though, including metal in an optical path results in decreasing optical quality factor caused by metal absorption. Moreover, metal contacts in an optical microcavity changing the mode structure. These new states, called Tamm plasmon polariton, may lead to an increase in the lasing threshold.[21,22]
Here, we introduce a new concept for structuring OLEDs which circumvents these obstructive effects. The emission zone is laterally expanded in the metal-free area by extending the layer sequence with transparent but still

Further author information: (Send correspondence to I.S.)
I.S.: E-mail: irma.slowik@iapp.de, Telephone: +49 351 463 38773

Organic Photonics VII, edited by David Cheyns, Pierre M. Beaujuge, Volker van Elsbergen, Jean-Charles Ribierre, Proc. of SPIE Vol. 9895, 989507 · © 2016 SPIE
CCC code: 0277-786X/16/$18 · doi: 10.1117/12.2228233

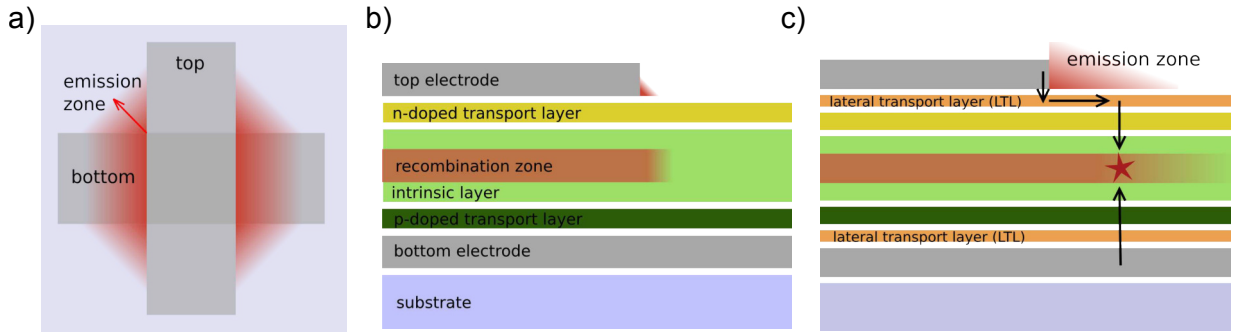

Figure 1. a) A plan view of the opaque electrodes, that are arranged perpendicular to each other (crossbar electrodes) on the substrate. b) In a standard OLED consisting of a p-doped/intrinsic/n-doped (pin) layer structure, emission takes mainly place in the overlap area of the electrode. c) When additional lateral transport layers (LTL) are inserted, substantial current flow extends to the metal-free region. The corresponding light emission (compare with a), laterally expands and can now leave the layer stack in both directions (top and bottom) since the LTL still has a good transmittance.

conductive layers (see Fig. 1 a)). Thus, a substantial emission takes place outside the original active area given by the overlap of the electrodes (compare Fig. 1 b) and c)). Furthermore, we can now avoid the use of transparent oxide electrode (e.g. indium-tin-oxide ITO) to contact our device by two highly conductive metal electrodes. In that sense, the new lateral transport layer (LTL) acts as a matching layer between the highly conductive but opaque electrodes and the less conductive organic transport layers. The lateral current transport is increased and the emission zone is extended into the metal-free areas without a strong increase in the absorption of the layer stack.

Such a concept enables integration into a pair of DBR mirrors to realize an organic vertical cavity surface emitting laser (VCSEL). As all layers are stacked in a sandwich architecture and can be structured by low-resolution shadow masks, our concept makes it interesting for further investigations. Even so, the current density strongly decays in the metal-free area, in the corners of the crossing electrode structure high intensities can be achieved. Hence, this structure could be sufficient for the realization of electrical pumping of an OSL, as high excitation densities are only required in the area comparable to the size of the transverse mode of the organic microcavity laser.[23]

2. EXPERIMENTAL

2.1 Sample Design and Preparation

We use high efficiency phosphorescent pin-OLEDs,[24] consisting of a 50 nm 2,2,7,7-tetrakis(N,N-di-p- methyl-phenylamino)-9,9-spirobifluorene (Spiro-TTB) hole transport layer, doped with 8 wt% 2,2-(perfluoronaphthalene-2,6-diylidene)-dimalononitrile (F_6-TCNNQ), a 10 nm 2,2,7,7-tetrakis- (N,N-diphenylamino)-9,9-spirobifluoren (Spiro-TAD) electron blocking layer, a 10 nm bis-(2-methyl-8-chinolinolato)-(4-phenyl-phenolato)-aluminium(III) ($BAlq_2$) hole blocking layer, a 50 nm Cs-doped 4,7-diphenyl-1,10- phenanthroline (BPhen) electron transport layer, and two 100 nm Al electrodes. The intrinsic emission layer consists of a 10 nm N,N-di(naphtalene-1-yl)-N,N-diphenylbenzidine (NPB) matrix doped with 10 wt% iridium(III)bis(2-methyldibenzo[f,h]quinoxaline) (acetylacetonate) ($Ir(MDQ)_2(acac)$).

To prove the expansion of the emission zone by lateral transport, for some samples an additional lateral transport layer is inserted between the electrode transport layer and the cathode. As lateral transport layer 10 nm of C_{60} doped with 16 wt% of the electron donor material (n-dopant) $W_2(hpp)_4$ (tetrakis(1,3,4,6,7,8-hexahydro-2Hpyrimido [1,2a] pyrimidinato)ditungsten (II)) is used.[25] All materials are purchased from commercial suppliers and purified further by vacuum gradient sublimation prior to use.

Organic materials are evaporated in a UHV-chamber (Kurt J. Lesker Co.) onto glass substrates. The thickness is measured in-situ using quartz crystal monitors. All samples are encapsulated under nitrogen atmosphere using glass lids and epoxy resin directly after fabrication.

2.2 Measurement

Current density-voltage-luminance characteristics of all samples are measured using a source-measure unit (Keithley SM2400), and a silicon photodiode.
The lateral emission of the OLEDs is investigated with an optical microscope (Nikon Eclipse High-resolution Microscope) combined with camera (Nikon DS-Fi1). Images of the lateral emission of the OLED are taken in darkness.

3. RESULTS

3.1 Investigation of the Lateral Emission

As the lateral distribution of the vertical current density cannot be directly measured, we investigate the spatially resolved emission pattern of different OLEDs outside the overlap area of the electrodes. To prove the idea of emission broadening by increasing lateral conductivity of the transport layers, we compare the spatially resolved emission of pin-OLEDs with (w/ LTL) and without additional lateral transport layer (w/o LTL).

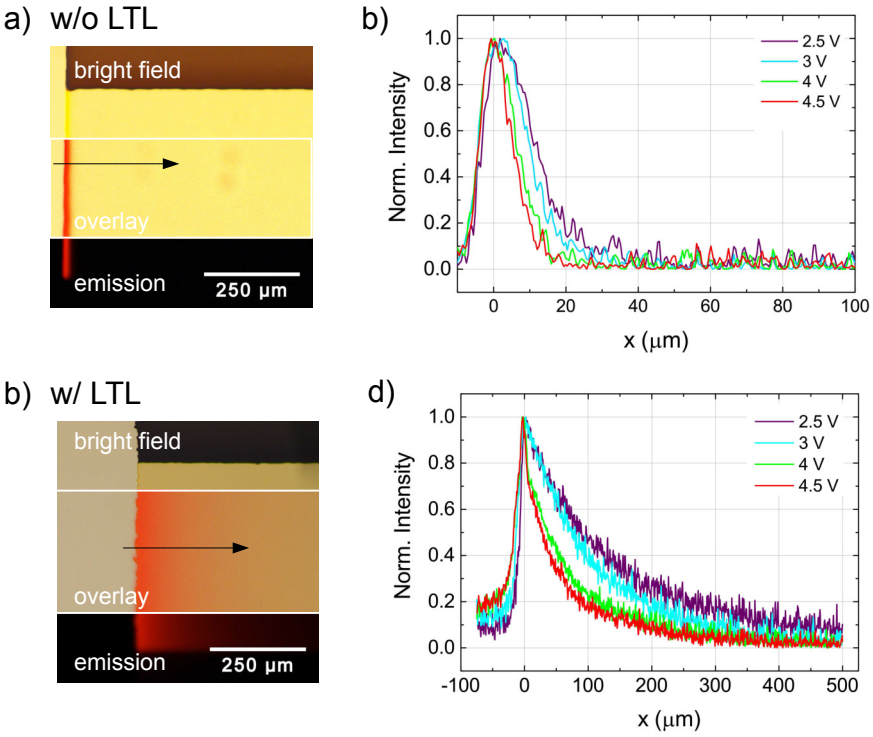

Figure 2. On the left side, the microscope image of the emission measured at 3 V of the crossbar structured OLEDs with opaque electrodes are depicted. In each case, on the top the bright field image is shown and on the bottom the emission. The middle part of the image visualizes the superposition of both measurements. The extracted profiles (direction indicated by the arrow) are presented on the right side. a) The emission of pin-OLED w/o LTL expands over a few micrometer in the metal-free area. b) In comparison, the same OLED stack with additional 10 nm of highly doped C_{60} w/ LTL between electron transport layer and cathode has an extension of the emission zone towards several 100 micrometers.

In Fig. 2, the emission micrographs of an OLED w/o LTL and an similar device with 10 nm of highly doped C_{60} w/ LTL are compared. In Fig. 2 a) and c) the bright-field microscope image with overlaying emission pattern measured at 3 V is depicted. To visualize the position of the emission on the sample, in the upper section of the picture only the bright field image and in the lower section only the emission measured is shown. The center part displays an overlay of both images. The right images b) and d) show the extracted emission profiles measured in the direction indicated by the arrows.
The lateral emission intensity of the OLED w/o LTL shows a strong decay outside of the contacted opaque electrode region. The shape of the decay can be described phenomenologically by an exponential function $I(x) \propto \exp(x/x_c)$, so that the decay length of the emission intensity x_c can be used as characteristic parameter for the description of the spatial emission distribution. Even though, the total emission intensity increases at higher external voltages, the emission decay length decreases. As shown in Fig. 2 b,) the emission intensity decays depending on the applied voltage 2.5 V - 4.5 V within a length scale of 11 µm to 5 µm, respectively. This dependency indicates that the described phenomenon is not caused by scattering of light at the electrode edge as the decay lengths depend on the applied voltage. In contrast to lateral charge transport in the LTL, the vertical current flow in the OLED exhibits a decreasing resistance with voltage, so that the lateral decay length of the emission decreases accordingly. Hence, the observed lateral broadening of the emission in the electrode-free area can be explained by lateral current transport within the transport layers.
For the OLED device w/ LTL, the area emission zone could be enhanced tremendously by one order of magnitude. A bright emission outside the electrodes can be seen in a range of several hundred micrometers. The decay length differs from 145 µm to 75 µm for the corresponding voltage range of 2.5 V to 4.5 V, respectively.

3.2 Simulation of the lateral current density distribution

A key issue for the new OLED concept is an understanding of the lateral distribution of the vertical current density within the organic layers outside the electrode area. For the design of an OLED with the appropriate layer stack, a quantitative description between the dimension of the emission zone and electrical properties of the organic layers is necessary. To reach high current densities at moderate voltages, low charge injection barriers as well as a low resistance by charge transport in vertical direction of the organic layer stack are required. However, high vertical conductivity results in a strong decay of the current density outside the metal covered area. On the other hand, for the electrical pumping, we need to provide the high excitations densities within an area comparable with the expansion of the transverse mode of an organic VCSEL.[23] Therefore, the conductivity of the LTL and the composition of the pin-OLED stack have to be designed well to achieve high current densities in a sufficient large area. Furthermore, due to the short lifetime of the singlet excitons, the high excitations densities have to be provided within the range of nanoseconds. As a fast turning-on of the current is crucial to suppress quenching mechanism induced by triplet exictons,[7] also the time-dependency of the current density in the organic layers has to be studied.
Here, we introduce a simulation of the time-dependent lateral distribution of a mesh vertical current density in the device using an equivalent circuit approach. The organic layers are divided into subunits which can be described by elements of an electric circuit. The current and voltage distribution of the network is solved by the freely available Software LTspice IV from Linear Technology*.
An an example, the circuit model for the lateral distribution of the vertical current flow between the crossbar electrodes (compare Fig. 1 a)) is depicted in Fig. 3. Hereby, the organic transport layers (p-doped, n-doped, LTL) are discretized in a network of Ohmic resistors characterized by sheet resistance of the associated transport layer R_{top}, R_{bot}. Since the emission layer has a much lower conductivity than the doped transport layers, only the sheet resistance of the doped layers have to be considered in the model. The sheet resistances are calculated from conductivity measurements of neat organic films σ and layer thickness t:

$$R_{\mathrm{top/bot}} = (\sigma \cdot t)^{-1} \tag{1}$$

For example, we use Spiro-TTB:F_6TCNNQ as p-doped transport layer with conductivities around $5 \cdot 10^{-5}$ S/cm, so that for a layer thickness of 50 nm it results in a sheet resistance of 400 MΩ/□. In comparison, the conductivity of the LTL is in the a range of 5 S/cm,[26] which gives sheet resistances of about 0.2 MΩ/□ . Consequently, in the

* http://www.linear.com/designtools/software/

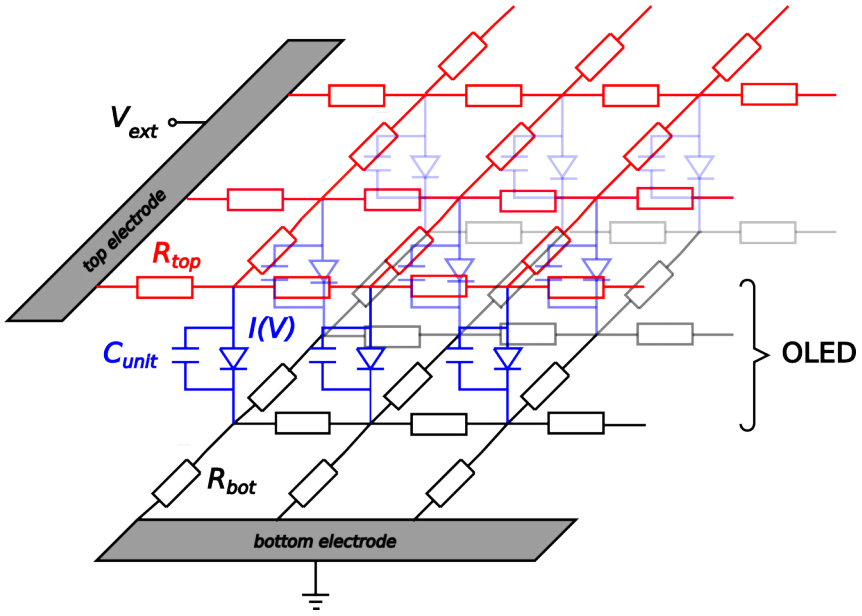

Figure 3. Schematic illustration of the equivalent circuit model. The organic layer stack is divided in subunits of electronic components. The lateral transport is described by a network of Ohmic resistors related to the sheet resistance of the transport layer R_{top}, R_{bot},. The OLED is represented by a diode, which is described by an arbitrary current source $I(V)$, and a parallel capacitor C_{unit}. In the depicted configuration, the network model of the organic layer in the upper left corner of the crossbar structure of Fig. 1 a) is presented.

presence of a highly conductive LTL, the current transport through the transport layers can be neglected.
The vertical current is described by a voltage-dependent current source $I(V)$ defined by the I-V characteristic of the OLED stack. For the implementation of the equivalent circuit simulation, the current-voltage dependency has to be written as algebraic function. We parametrize the I-V characteristic using a power law $I(V) = I_0 \cdot V^{\alpha}$ as shown in Fig. 4. As different parts of the curve have different slopes, we combine different power law functions by an harmonic mean to an envelope describing a broaden voltage range. At high excitations the power law would merge into a quadratic law due to the space charge limitation of the current in organic semiconductors.
Besides the lateral emission profile, the time-dependent behavior of the current density distribution is of interest because potential application in an organic laser requires pulsed operation. In order to simulate the turn-on characteristic of the current, the capacitance of the subunits are described by a capacitor parallel to the current source. To calculate the capacitance of a single circuit element C_{unit}, the capacitance C_{OLED} of full OLED device with an electrode area A_{OLED} of 0.07 mm^2 is measured by impedance spectroscopy and normalized to a single circuit element area A_{unit}. The area of an single circuit element A_{unit} is defined by the length x and width y of the simulated domain divided by the discretization steps for both dimensions n_x, n_y:

$$A_{\mathrm{unit}} = \frac{x \cdot y}{n_x \cdot n_y}. \tag{2}$$

The external voltage is applied between the edges of the bottom and the top layer depending on the device geometry, i.e. in above described crossbar structure (see Fig. 1 a)) between the front side of the bottom electrode and the left side of the top electrode. Besides the shown example, the equivalent circuit approach can be used to simulate multiple device structures and material parameters. For example, the in Sec. 3.1 investigated lateral emission along the bottom electrode can be described by a network with a highly conductive transport layer at the bottom layer defined by the sheet resistance of the metal. Alternatively, since the lateral current distribution is limited by the less conductive transport layer, the distribution of the vertical current density is equivalent to a symmetric structure with equal sheet resistances R_{top}, R_{bot} determined by the less conductive side.
The simulated current density distribution is compared with the lateral emission intensity in the metal-free area. In Fig. 4 b), the dependency of the luminescence on the current densities of the OLED w/o LTL (compare

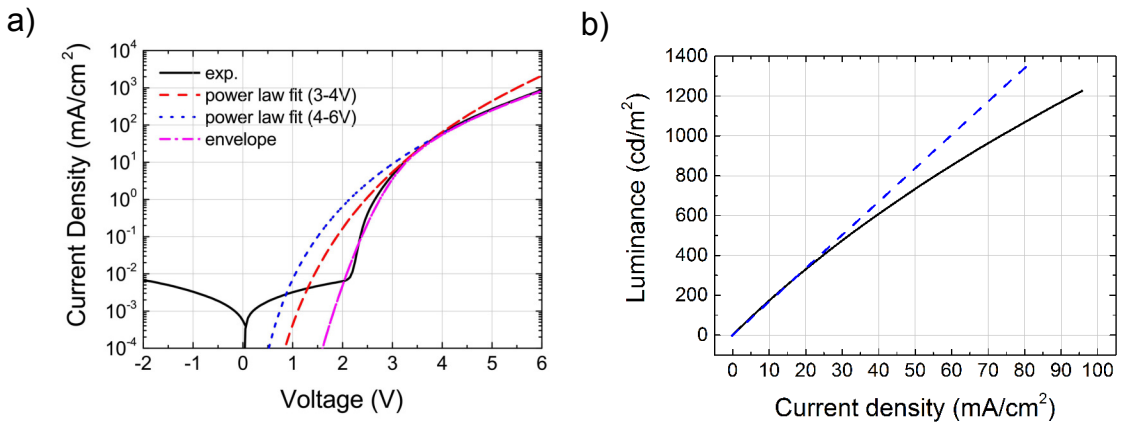

Figure 4. a) The I-V characteristic of an OLED w/o LTL with an area of 0.07 mm^2 is shown. The current-voltage characteristic is fitted with two power law functions $I(V) = I_0 \cdot V^\alpha$ in the voltage range between 2 - 3 V ($I_0 = 3 \cdot 10^{-11}$ mA/V$^\alpha$,$\alpha = 17.4$) and the 3 - 6 V ($I_0 = 5 \cdot 10^{-6}$ mA/V$^\alpha$,$\alpha = 6.5$). An envelope is calculated by the harmonic mean of both functions. b) The luminance-current density characteristic of the OLED in a) is depicted. At low excitation below 30 mA/cm^2, the luminescence intensity scales approximately proportional to the current density (dashed blue line).

Fig. 4 a)) is depicted showing an almost linear behavior at low current densities up to 30 mA/cm^2. Therefore, a direct comparison between the normalized emission intensity and the normalized current density can be drawn. At higher excitation levels the emission intensity does not scale proportionally with the current annihilation processes.

3.3 Comparison between Simulation and Experiment

As verification of our earlier introduced equivalent circuit model (see Sec. 3.2), we compare the experimental data with the simulated lateral distribution of the vertical current density. A comparison is drawn between the emission image from the microscope in Fig. 5 a) and and the current density distribution in Fig. 5 b). Profiles of the normalized emission intensity are extracted and compared with profiles of the current density decay generated with the equivalent circuit simulation (see Fig. 5 c)).

As an example, we show the analysis of an OLED w/ LTL of 10 nm of highly doped C_{60} depicted in Fig. 2 measured at an operating voltage of 3 V. At the metal edge, the emission intensity has a maximum and decreases with increasing distance to the top electrode. The strong decay takes place within in the first 100 µm. Still, emission can be detected over hundreds of micrometers. From Fig. 5 c) it can be seen that also the shape of the simulated profiles coincides with the measured results. The decay lengths of the emission intensity of 95 µm matches with the one of the vertical current density distribution of around 110 µm. A direct comparison between both values can be done as the luminescence scales linear with the current for small current densities. The simulation also gives a quantitative description for the decrease in the emission decay lengths for higher driving voltages of the OLED already seen in Fig. 2.

Hence, the experimental findings confirm the feasibility of an equivalent circuit model as a description of the organic layer stack calculating the current flow in the active area of the device. As the model parameters correspond well with the experimentally determined values, we can use the equivalent circuit model as a tool to test different material parameters to get an understanding of the requirements for the electrical pumping of an OSL. Furthermore, by measuring the emission intensity decay, a conclusion about the material properties of the transport layers of the OLED can be drawn.

To reach current densities above the lasing threshold in an metal-free area of the size of the transverse mode of an organic VCSEL, the right match of material properties of the lateral transport layer have to be fulfilled.[6,23] On the one hand, the resistance by vertical charge transport of the OLED should be low to enable high current densities. On the other hand, high vertical conductivities result in a strong decrease of the current density in the metal-free area. Therefore, an LTL with a sufficient conductivity has to be found, still providing low absorption

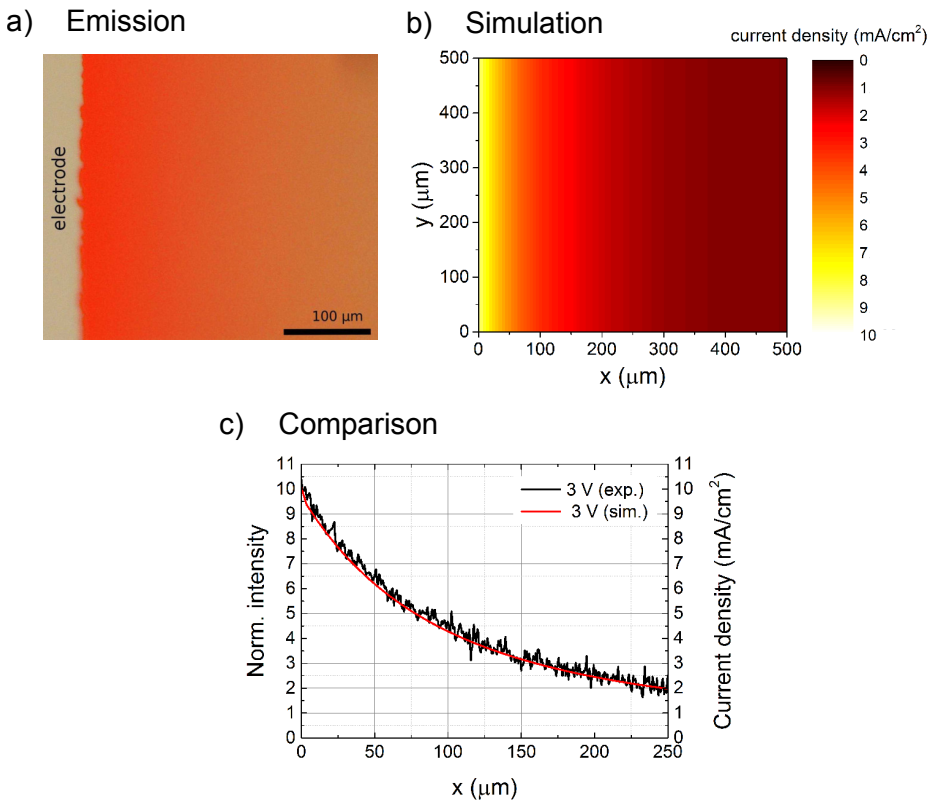

Figure 5. a) Microscope image of the lateral emission of an OLED w/ LTL 10 nm of highly doped C_{60} measured at 3 V (compare Fig. 2 b)) close to the edge of the top electrode. b) As comparison, the simulated current distribution by an equivalent circuit simulation is shown. c) Comparison of extracted profiles of the lateral emission in a) and current density in b).

in the visible spectral range. Such a highly conductive and transparent LTLs can be realized e.g. by highly doped organic layers,[26] conducting polymers,[27] thin metal films[28] or conductive 2D materials such as graphene.[29–31] As can be seen in Fig. 6 a), the decay length of the current density strongly depends on the conductivity of the transport layers. In the shown example (compare Fig. 2) of an LTL made by highly doped C_{60} ($\sigma \approx 5$ S/cm), an emission intensity decay length of about 100 µm is achieved. Changing the material of the LTL, the emission zone could be extended even further. It is shown already that with PEDOT:PSS, conductivities of more than 1000 S/cm can be realized.[17] Including such a layer in the previously used OLED stack, decay lengths in the range of more than 1 mm should be achieved for standard driving voltages. The drop of the lateral emission intensity over a standard pixel size of several hundred micrometers would be less than 20%. Thus, including a highly conductive matching layer between transport layers and electrodes opens up the possibility for the development of a fully organic LED.

In order to predict the lateral distribution of the vertical current density at high excitations, we can simulate the current density decay length for high driving voltages, e.g. 100 V see Fig. 6 a). To achieve a localization of the high current densities above 1 kA/cm^2 in the range of the mode diameter of an organic VCSEL[23] of a few micrometers at least conductivities of 1 S/cm are required. Hence, already the presented LTL made of highly doped C_{60} is a promising candidate to provide high current densities in a sufficient large area for electrical pumping and still having low absorption in the red wavelength regime.[28] Using PEDOT:PSS, the active area for electrical pumping could be further enhanced to several tens of micrometers.

To achieve high excitation densities, pulsed excitation of the OLED short pulses in the range of nanoseconds are required to reduce Joule heating[32] as well as undesired effects caused by triplet excitons like singlet-triplet

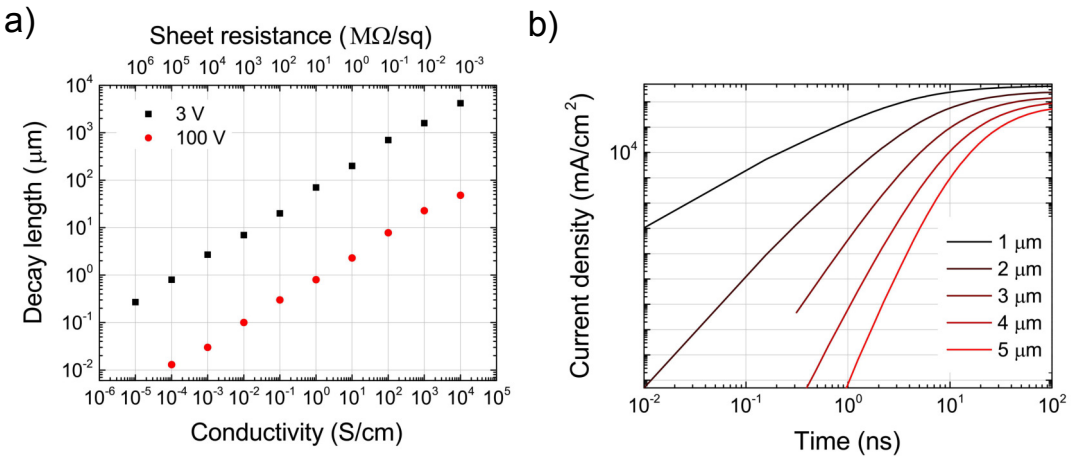

Figure 6. a) The graph depicts the simulated dependence between the decay length of the current density in the metal free area on the conductivity of the lateral transport layer (10 nm) for the OLED with an I-V characteristic shown in Fig. 4 a) at the driving voltage of 3 V (red dots) and 100 V (black square). The decay length strongly depends on the driving voltage due to the non-linear I-V curve. b) The transient current density for a device with an LTL of 10 nm highly doped C_{60} is simulated at 100 V at different distances to the electrode edge (1 µm to 5 µm). After 300 ns, the maximum current density is reached within the entire range. That means the complete area required for the electrical pumping of an organic VCSEL mode is switched on.

quenching as well as triplet absorption.[7,12,16] Therefore, we investigate the transient current density of the new OLED structure at different distances from the metal edge to get an understanding, how fast the area of the device required for electrical pumping of a laser mode can be switched on by the LTL. In Fig. 6 b) the time-dependent current density of an OLED w/ LTL of 10 nm of highly doped C_{60} at a driving voltage of 100 V is simulated for different distances to the electrode edge. Due to the sheet resistance of the LTL and the capacitance of the OLED, the current density increases within a typical RC time, here in the range of 10 ns - 100 ns. In the shown example, the estimated lasing threshold of 1 kA/cm^2 can be achieved in an area with an diameter of 4 µm in less than 100 ns. The steady state is reached around 300 ns after the turn-on of the voltage. From this, we can conclude, that the introduced concept is suitable for excitation with pulse length in the range of several hundred nanoseconds. Further downscaling of the turn-on time of the device can be achieved using LTL with higher conductivity allowing even shorter pulse lengths, e.g. PEDOT:PSS reducing the turn-on time to approx. 25 ns, or applying larger voltages.

Still, it has to be taken into account that for high excitations, role-off mechanism like singlet-triplet annihilation and polaron annihilation plays an dominant role, resulting in an increase in lasing threshold.[6,15] At present, the obstacles for the electrical pumping are not given by the structure but the limitation of the organic materials in terms of singlet lifetime, quenching mechanism and electrical transport properties. Nevertheless, due to large variety of potential organic materials,[33] the introduced concepts seem to be a promising solution towards the realization of an electrically driven OSL.

4. SUMMARY AND OUTLOOK

In summary, we introduce a new OLED structure, where the emission is expanded towards the metal-free area by additional highly conductive but still transparent lateral transport layers. Thus, absorption at the metal contact can be circumvented. By measuring the lateral emission, we proved that by inserting a layer of 10 nm, highly doped C_{60} increases the emission zone up to several hundred micrometers outside the electrode.

We confirm experimental findings by simulations using an equivalent circuit model discretizing the organic layer stack in subunits consisting of electric circuit elements. With this approach, a large variety of OLED structures and organic devices can be described. The equivalent circuit model gives a fast and simple access for the simulation of the time-dependent current-voltage distribution within the organic layer stack. We used the

simulation to get an insight into the lateral distribution of the vertical current densities in the metal-free area depending on the material properties of the OLED stack. Thereby, it has been proven that using conventional organic materials high excitations in the area of the mode volume of an organic VCSEL could be achieved.
As the new structure is easy to integrate into an organic microcavity as well as being compatible with the conventional OLED processing technology, it provides a feasible framework for electrical pumping of an OSL. Further attempts to improve the structure can be done by suppressing vertical current flow in the active area between the electrodes to reduce Joule heating of the device.

ACKNOWLEDGMENTS

This work is partly supported by the German Research Foundation (DFG) within the Cluster of Excellence 'Center for Advancing Electronics Dresden' and the DFG project LE 747/53-1.

REFERENCES

[1] Forrest, S. R., "The path to ubiquitous and low-cost organic electronic appliances on plastic," *Nature* **428**(6986), 911–918 (2004).
[2] Kamtekar, K. T., Monkman, A. P., and Bryce, M. R., "Recent advances in white organic light-emitting materials and devices (WOLEDS)," *Advanced Materials* **22**(5), 572–582 (2010).
[3] Tang, C. W. and Vanslyke, S. A., "Organic electroluminescent diodes," *Applied Physics Letters* **51**(12), 913–915 (1987).
[4] Meerheim, R., Lüssem, B., and Leo, K., "Efficiency and stability of p-i-n type organic light emitting diodes for display and lighting applications," *Proceedings of the IEEE* **97**(9), 1606–1626 (2009).
[5] Reineke, S., Lindner, F., Schwartz, G., Seidler, N., Walzer, K., Lüssem, B., and Leo, K., "White organic light-emitting diodes with fluorescent tube efficiency.," *Nature* **459**(7244), 234–8 (2009).
[6] Gärtner, C., Karnutsch, C., Lemmer, U., and Pflumm, C., "The influence of annihilation processes on the threshold current density of organic laser diodes," *Journal of Applied Physics* **101**, 023107 (2007).
[7] Kasemann, D., Brückner, R., Fröb, H., and Leo, K., "Organic light-emitting diodes under high currents explored by transient electroluminescence on the nanosecond scale," *Physical Review B* **84**(11), 115208 (2011).
[8] Murawski, C., Leo, K., and Gather, M. C., "Efficiency roll-off in organic light-emitting diodes," *Advanced Materials* **25**(47), 6801–6827 (2013).
[9] Tessler, N., Harrison, N. T., Thomas, D. S., and Friend, R. H., "Current heating in polymer light emitting diodes," *Applied Physics Letters* **73**(6), 732–734 (1998).
[10] Yoshida, K., Nakanotani, H., and Adachi, C., "Effect of Joule heating on transient current and electroluminescence in p-i-n organic light-emitting diodes under pulsed voltage operation," *Organic Electronics* **31**, 287–294 (2016).
[11] Fischer, A., Pahner, P., Lüssem, B., Leo, K., Scholz, R., Koprucki, T., Fuhrmann, J., Gärtner, K., and Glitzky, A., "Self-heating effects in organic semiconductor crossbar structures with small active area," *Organic Electronics* **13**(11), 2461–2468 (2012).
[12] Baldo, M., Holmes, R., and Forrest, S., "Prospects for electrically pumped organic lasers," *Physical Review B* **66**(3), 035321 (2002).
[13] Samuel, I. D. W. and Turnbull, G. a., "Organic semiconductor lasers," *Chemical reviews* **107**(4), 1272–95 (2007).
[14] Chenais, S. and Forget, S., "Recent advances in solid-state organic lasers," *Polymer International* **61**(3), 390–406 (2013).
[15] Setoguchi, Y. and Adachi, C., "Suppression of roll-off characteristics of electroluminescence at high current densities in organic light emitting diodes by introducing reduced carrier injection barriers," *Journal of Applied Physics* **108**(6), 064516 (2010).
[16] Hayashi, K., Nakanotani, H., Inoue, M., Yoshida, K., Mikhnenko, O., Nguyen, T. Q., and Adachi, C., "Suppression of roll-off characteristics of organic light-emitting diodes by narrowing current injection/transport area to 50 nm," *Applied Physics Letters* **106**(9), 093301 (2015).

[17] Kuwae, H., Nitta, A., Yoshida, K., Kasahara, T., Matsushima, T., Inoue, M., Shoji, S., Mizuno, J., and Adachi, C., "Suppression of external quantum efficiency roll-off of nanopatterned organic-light emitting diodes at high current densities," *Journal of Applied Physics* **118**(15), 155501 (2015).

[18] Zhao, Y., Yun, F., Wu, Z., Li, Y., Jiao, B., Huang, Y., Li, S., Feng, L., Guo, M., Ding, W., Zhang, Y., and Dou, J., "Efficiency roll-off suppression in organic light-emitting diodes at high current densities using gold bowtie nanoantennas," *Applied Physics Express* **9**, 022101 (2016).

[19] Nakanotani, H., Oyamada, T., Kawamura, Y., Sasabe, H., and Adachi, C., "Injection and transport of high current density over 1000 A/cm2 in organic light emitting diodes under pulse excitation," *Japanese Journal of Applied Physics* **44**(6 A), 3659–3662 (2005).

[20] Matsushima, T. and Adachi, C., "Observation of extremely high current densities on order of MA/cm 2 in copper phthalocyanine thin-film devices with submicron active areas," *Japanese Journal of Applied Physics* **46**(45-49), L1179–L1181 (2007).

[21] Brückner, R., Sudzius, M., Hintschich, S. I., Fröb, H., Lyssenko, V. G., and Leo, K., "Hybrid optical Tamm states in a planar dielectric microcavity," *Physical Review B* **83**(3), 033405 (2011).

[22] Brückner, R., Lyssenko, V., Hofmann, S., and Leo, K., "Lasing of Tamm states in highly efficient organic devices based on small-molecule organic semiconductors," *Faraday Discussions* **174**, 183–201 (2014).

[23] Ujihara, K., "Spontaneous emission and the concept of effective area in a very short cavity with plane-parallel dielectric mirrors," *Japanese Journal of Applied Physics* **30**(12A), 3388–3398 (1991).

[24] Murawski, C., Liehm, P., Leo, K., and Gather, M. C., "Influence of cavity thickness and emitter orientation on the efficiency roll-off of phosphorescent organic light-emitting diodes," *Advanced Functional Materials* **24**(8), 1117–1124 (2014).

[25] Menke, T., Ray, D., Meiss, J., Leo, K., and Riede, M., "In-situ conductivity and Seebeck measurements of highly efficient n-dopants in fullerene C60," *Applied Physics Letters* **100**, 093304 (2013).

[26] Schubert, S., Kim, Y. H., Menke, T., Fischer, A., Timmreck, R., Müller-Meskamp, L., and Leo, K., "Highly doped fullerene C60 thin films as transparent stand alone top electrode for organic solar cells," *Solar Energy Materials and Solar Cells* **118**, 165–170 (2013).

[27] Kim, Y. H., Sachse, C., Machala, M. L., May, C., Müller-Meskamp, L., and Leo, K., "Highly Conductive PEDOT : PSS Electrode with Optimized Solvent and Thermal Post-Treatment for ITO-Free Organic Solar Cells," *Advanced Functional Materials* **21**(6), 1076–1081 (2011).

[28] Schubert, S., Meiss, J., Müller-Meskamp, L., and Leo, K., "Improvement of Transparent Metal Top Electrodes for Organic Solar Cells by Introducing a High Surface Energy Seed Layer," *Advanced Energy Materials* **3**(4), 438–443 (2013).

[29] Kim, K., Zhao, Y., Jang, H., Lee, S., Kim, J., Ahn, J.-H., Kim, P., Choi, J.-Y., and Hong, B., "Large-scale pattern growth of graphene films for stretchable transparent electrodes," *Nature* **457**(7230), 706–710 (2009).

[30] Bonaccorso, F., Sun, Z., Hasan, T., and Ferrari, A. C., "Graphene Photonics and Optoelectronics," *Nature Photonics* **4**(9), 611–622 (2010).

[31] Lee, B. H., Lee, J. H., Kahng, Y. H., Kim, N., Kim, Y. J., Lee, J., Lee, T., and Lee, K., "Graphene-conducting polymer hybrid transparent electrodes for efficient organic optoelectronic devices," *Advanced Functional Materials* **24**(13), 1847–1856 (2014).

[32] Fischer, A., Pahner, P., Lüssem, B., Scholz, R., Leo, K., Koprucki, T., Gärtner, K., and Glitzky, A., "Self-Heating, Bistability, and Thermal Switching in Organic Semiconductors," *Physical Review Letters* **110**(12), 126601 (2013).

[33] Nakanotani, H., Akiyama, S., Ohnishi, D., Moriwake, M., Yahiro, M., Yoshihara, T., Tobita, S., and Adachi, C., "Extremely low-threshold amplified spontaneous emission of 9,9'-spirobifluorene derivatives and electroluminescence from field-effect transistor structure," *Advanced Functional Materials* **17**(14), 2328–2335 (2007).